Chaotic mixing due to a spatially periodic three-dimensional flow (Turbulence Transport, Diffusion and Mixing)

AUTHOR(S):

Mizuno, Yoshinori; Funakoshi, Mitsuaki

数理解析研究所講究録 1339 巻 2003 年 23-34

Chaotic mixing due to a spatially periodic three-dimensional flow

京都大学大学院 情報学研究科
水野吉規 (Yoshinori Mizuno), 船越満明 (Mitsuaki Funakoshi)
Graduate School of Informatics, Kyoto University

1 Introduction

Mixing of a fluid has been studied on the basis of theories of dynamical systems. It is known that Stokes flow or a flow with low Reynolds numbers can mix the fluid well within a region where the trajectories of fluid particles are chaotic, called chaotic region hereinafter, even if the velocity field itself behaves regularly or is steady if it is three-dimensional (Ottino (1989), Ottino (1990) and Aref (1990)). Partitioned pipe mixer (PPM) is one of the systems studied from the viewpoint of dynamical systems (Khakhar et al. (1987), Ling (1993) and Meleshko et al. (1999)). This system first introduced by Khakhar et al. originally consists of an infinitely long cylinder and plane plates of the same length fixed orthogonally to each other. Figure 1(a) shows schematic view of one period of the original PPM. Rotation of the cylindrical wall and pressure gradient in the axial direction cause a flow in this system. In Khakhar et al. (1987) and Meleshko et al. (1999) that are based on approximate velocity fields, it is shown that chaotic mixing can occur in this system. Mizuno and Funakoshi (2002) then generalized the PPM so that the ratio of the lengths of neighboring plates or the angle between them can be changed. One period of the generalized PPM is shown in Fig.1(b). In the examination of the mixing of a fluid within the generalized PPM, it is shown that the chaotic region can occupy the almost whole region if the ratio or the angle is appropriately changed.

Generally, there exists regions that do not mix quickly with the surrounding fluid even within chaotic regions. It is confirmed by calculating the distribution of stretching rate of fluid elements(Muzzio et al. (1991)). Capturing the existence and distribution of these regions needs to understand the mixing process there. In the experimental study on the mixing in PPM by Kusch and Ottino (1992), it was noted that the separation of the fluid by the leading edges of plane plates is a contributing mechanism to the mixing. Although they also noted that chaos can occur without any cutting mechanism, the consideration of this mechanism which static mixers commonly possess is expected to be a useful approach to understanding the mixing process in these mixers. Hence, Mizuno and Funakoshi (2002) focused on the separation of the flow by the leading edges, and examined the efficiency of the mixing within the chaotic region by introducing *the lines of separation*, defined as the set of cross-sectional initial locations of fluid particles which move to one of the leading edges of the plates within a specified period. Consequently, it was found that the lines of separation plays an important role in the estimation of the

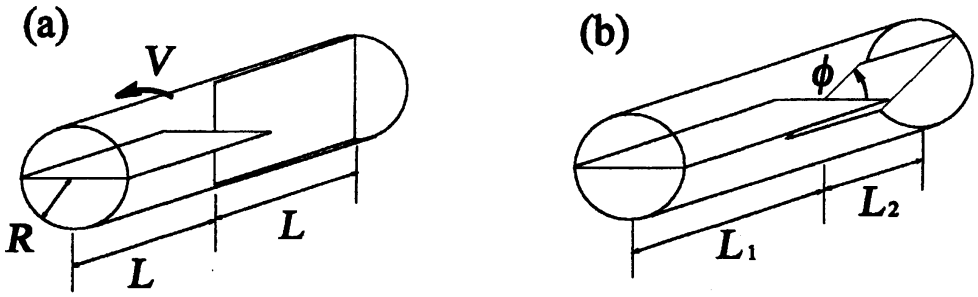

Figure 1: Schematic view of PPMs. (a) Original PPM. (b) Generalized PPM.

mixing performance in a few periods.

However, it should be noted that the velocity fields in the preceding studies are assumed to be independent of the axial coordinate within each region around each plate, hereinafter an element, and to change discontinuously at the cross-sections between neighboring elements. The validity of these assumptions is not clear. Therefore, we here calculate the velocity field numerically without these assumptions, and examine the mixing of a fluid, especially in one period. Furthermore, we will show that the consideration of the separation by the leading edges help to understand the mixing process within the chaotic region.

2 Velocity field in PPM

Let (r, θ) be the polar coordinates in the cross-sectional direction of a pipe with radius R, and z be the coordinate in its axial direction. The cylindrical wall $r = R$ of the pipe is assumed to rotate at constant velocity V. Horizontal plates of length L_1 expressed by $\{ (r, \theta, z) \mid 0 \leq r \leq R,\ \theta = 0 \text{ or } \pi,\ k(L_1 + L_2) < z < k(L_1 + L_2) + L_1 \}$ and vertical plates of length L_2 expressed by $\{ (r, \theta, z) \mid 0 \leq r \leq R,\ \theta = \pi/2 \text{ or } 3\pi/2,\ k(L_1 + L_2) + L_1 < z < (k+1)(L_1 + L_2) \}$ are placed alternately within this pipe, where $k = 0, \pm 1, \pm 2, \cdots$.

Assuming the spatial periodicity in the axial direction of the system, we take the flow region as

$$\mathrm{D} = \{ (r, \theta, z) | 0 < r < R,\ 0 < \theta < 2\pi, : 0 < z < L_1 + L_2 \}.$$

We here assume the steady Stokes flow in region D. If the velocity field and pressure are $\boldsymbol{v} = (v_r, v_\theta, v_z)$ and P, respectively, the equation of continuity and the Navier-Stokes equation under the Stokes approximation are given by

$$\nabla \cdot \boldsymbol{v} = 0, \tag{1}$$

$$-\frac{\partial P}{\partial r} + \beta \left(\frac{\partial^2 v_r}{\partial r^2} + \frac{1}{r}\frac{\partial v_r}{\partial r} + \frac{1}{r^2}\frac{\partial^2 v_r}{\partial \theta^2} + \alpha^2 \frac{\partial^2 v_r}{\partial z^2} - \frac{v_r}{r^2} - \frac{2}{r^2}\frac{\partial v_\theta}{\partial \theta} \right) = 0, \tag{2}$$

$$-\frac{1}{r}\frac{\partial P}{\partial \theta}+\beta\left(\frac{\partial^2 v_\theta}{\partial r^2}+\frac{1}{r}\frac{\partial v_\theta}{\partial r}+\frac{1}{r^2}\frac{\partial^2 v_\theta}{\partial \theta^2}+\alpha^2\frac{\partial^2 v_\theta}{\partial z^2}-\frac{v_\theta}{r^2}+\frac{2}{r^2}\frac{\partial v_r}{\partial \theta}\right)=0, \tag{3}$$

$$-\alpha^2\frac{\partial P}{\partial z}+\beta\left(\frac{\partial^2 v_z}{\partial r^2}+\frac{1}{r}\frac{\partial v_z}{\partial r}+\frac{1}{r^2}\frac{\partial^2 v_z}{\partial \theta^2}+\alpha^2\frac{\partial^2 v_z}{\partial z^2}\right)=0, \tag{4}$$

$$\boldsymbol{v}=\boldsymbol{0} \quad \text{on} \quad \begin{cases} \theta=0,\pi, & 0<z<l_1, \\ \theta=\frac{\pi}{2},\frac{3\pi}{2}, & l_1<z<2, \end{cases} \tag{5}$$

$$v_r, v_z=0,\ v_\theta=1 \quad \text{on} \quad r=1, \tag{6}$$

$$\boldsymbol{v}(z=0)=\boldsymbol{v}(z=2), \quad P(z=0)=P(z=2)+1, \tag{7}$$

where

$$\alpha=\frac{R}{(L_1+L_2)/2}, \quad \beta=\frac{\mu V}{RP_d}, \quad l_1=\frac{L_1}{(L_1+L_2)/2},$$

and we non-dimensionalized the length in the cross-sectional direction, length in the axial direction, velocities in the cross-sectional direction, velocity in the axial direction and pressure with R, $(L_1+L_2)/2$, V, $(L/R)V$ and P_d, respectively. Here μ and P_d are the viscosity of the fluid and the pressure drop during one period in the axial direction, respectively. The parameter α is the aspect ratio of the system, and β is the ratio of the representative velocity of the cross-sectional flow due to the rotation of the cylindrical wall to that of the axial flow due to the pressure gradient.

The boundary value problem (1)–(7) is solved numerically. We here assume that the velocity and pressure fields have the symmetry with respect to the rotation by π around the z axis. Hence, we restrict the range of θ to $(0,\pi)$. Since the velocity field changes largely in the regions around $z=0$, l_1 and 2, we use a coordinate ζ that is stretched within these regions instead of z. The relation between z and ζ is given by

$$z=\begin{cases} p\left\{\left(\frac{1}{2}+\varepsilon\right)\pi\zeta-\frac{1}{2}\cos(\pi\zeta)\sin(\pi\zeta)\right\}, & 0<\zeta<1 \\ q\left\{\left(\frac{1}{2}+\varepsilon\frac{p}{q}\right)\pi(\zeta-1)-\frac{1}{2}\cos(\pi(\zeta-1))\sin(\pi(\zeta-1))\right\}+l_1, & 1<\zeta<2, \end{cases} \tag{8}$$

where

$$p=\frac{l_1}{\pi/2+\varepsilon\pi}, \quad q=\frac{2-l_1+4\varepsilon(1-l_1)}{\pi/2+\varepsilon\pi},$$

and ε is a non-zero value chosen so that $|\frac{dz}{d\zeta}|\neq 0$ at $\zeta=0,1,2$. We choose $\varepsilon=0.5$ for $a=1.0$, $\varepsilon=0.3$ for $a=1.85$, 2.33, and $\varepsilon=0.2$ for $a=3.0$. We obtain the velocity field satisfying Eqs.(1)–(7) as the steady solution to

$$\nabla\cdot\boldsymbol{v}=0, \quad \text{and,} \quad \frac{\partial \boldsymbol{v}}{\partial t}=-\text{grad}P+\beta\nabla^2\boldsymbol{v}, \tag{9}$$

with boundary conditions (5)–(7) by SMAC method (Ferziger and Perić (1999)) with finite difference method on a staggered grid. The accuracy of the discretization is second

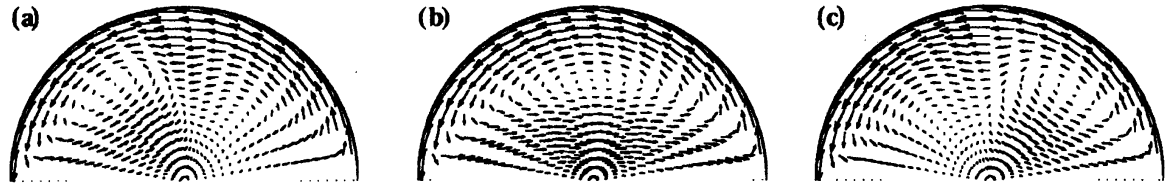

Figure 2: Cross-sectional flow. $\alpha = 0.5$, $\beta = 0.03$ and $a = 1$. (a) $z = 0.1l_1$, (b) $z = 0.5l_1$, (c) $z = 0.9l_1$.

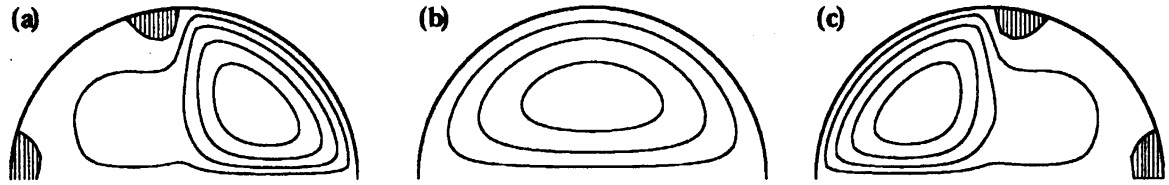

Figure 3: Contours of axial velocity. $\alpha = 0.5$, $\beta = 0.03$ and $a = 1$. (a) $z = 0.1l_1$, (b) $z = 0.5l_1$, (c) $z = 0.9l_1$.

order, and the number of the grid points is $40 \times 40 \times 80$.

The cross-sectional flow and contours of the axial velocity at three axial positions are shown in Figs.2 and 3, respectively. Only the upper parts are shown in these figures. The wall rotation generates vortical flows in the cross-sectional direction at all the axial positions, as seen in Fig.2. In the axial direction, although total flux is positive because of the pressure drop in the axial direction, we can recognize backward flows near the ends of the plate, as shown in Figs.3(a) and (c), where backward flows occur within the hatched regions. These backward flows are caused by the wall rotation. In contrast to the approximate velocity fields used in the preceding studies, there can be orbits wandering between neighboring elements for a long time and also closed orbits because of the backward flow. Although the former orbits are chaotic, they stay within a pair of neighboring elements for a long time. Since such orbits are not appropriate for a mixing device, we choose the small value of β so that the region in which the axial velocity has backward direction is small. Backward flow was also observed in the experimental study by Kusch and Ottino (1992).

3 Results

Once a velocity field is obtained, we can track the trajectories of fluid particles by integrating ordinary differential equation

$$\frac{d\boldsymbol{x}(t)}{dt} = \boldsymbol{v}(\boldsymbol{x}(t)), \tag{10}$$

where $\boldsymbol{x}(t)$ is the position of a fluid particle, and t is the time non-dimensionalized by R/V.

Since the velocity is periodic in the axial direction, we here consider a map defined as

$$M_{z_0} : (r, \theta) \mapsto (r(T(r, \theta)), \theta(T(r, \theta))), \tag{11}$$

where $T(r, \theta)$ is the minimum time which satisfies

$$\int_0^{T(r,\theta)} v_z(t)dt = 2, \tag{12}$$

on the trajectory of Eq.(10) starting from (r, θ, z_0) at $t = 0$. This mapping represents the cross-sectional movement of the fluid particle initially located at (r, θ) on $z = z_0$ after one period in the axial direction, and $T(r, \theta)$ is the time required for the movement.

3.1 Poincaré sections

In the preceding studies based on the approximate velocity field and also in the experimental study, tubular invariant sets of the trajectories, called KAM-tubes hereinafter, that prevent the transport of fluid particles between its inside and outside were recognized for some sets of the values of system parameters. We can also find them in Poincaré sections based on the numerically obtained velocity field. The Poincaré sections associated with $M_{l_1/2}$ for three values of β with α and a fixed to 0.5 and 1.0, respectively, are shown in Fig.4. It is found that the islands can shrink or disappear as β increases. Figures 5 and 6 show the Poincaré sections for three values of a with β fixed to 0.01 and 0.03, respectively. For $\beta = 0.01$, some islands disappear as a increases from 1.0. However, other islands remain and become larger. On the other hand, for $\beta = 0.03$, no recognizable island exists for $a = 2.33$ and 3.0 although we observe a few islands for $a = 1.0$, as shown in Fig.6. This shows that changing a can erase the KAM-tubes for appropriate values of β.

Although understanding the mixing process within chaotic region is also important issue for applications, we cannot obtain information on it from these Poincaré sections. Therefore, we next examine the mixing process within the chaotic region by introducing the lines of separation.

3.2 Lines of separation and mixing process in chaotic region

We introduce the lines of separation, $U_{z_0}^n$, in order to examine the mixing of a fluid in the chaotic region. Before giving the definition of the lines of separation, we introduce

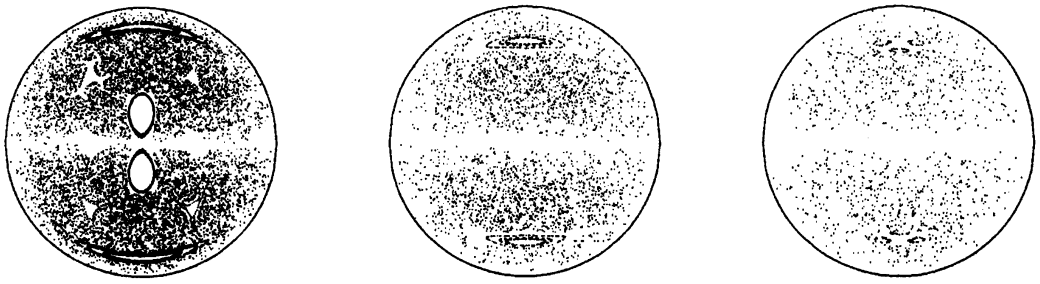

(a) (b) (c)

Figure 4: Poincaré sections based on $M_{l_1/2}$. $\alpha = 0.5$ and $a = 1.0$. (a) $\beta = 0.01$, (b) $\beta = 0.03$, (c) $\beta = 0.1$. 83 fluid particles are initially placed on square grid points of interval 0.1 in the first quadrant. Their trajectories are calculated up to $t = 100$.

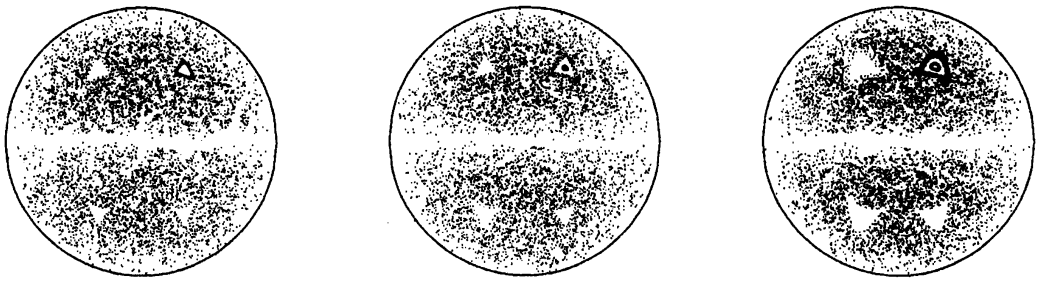

(a) (b) (c)

Figure 5: Poincaré sections based on $M_{l_1/2}$. $\alpha = 0.5$ and $\beta = 0.01$. (a) $a = 1.85$, (b) $a = 2.33$, (c) $a = 3.0$. The initial locations of fluid particles and the period of plotting are the same as Fig.4.

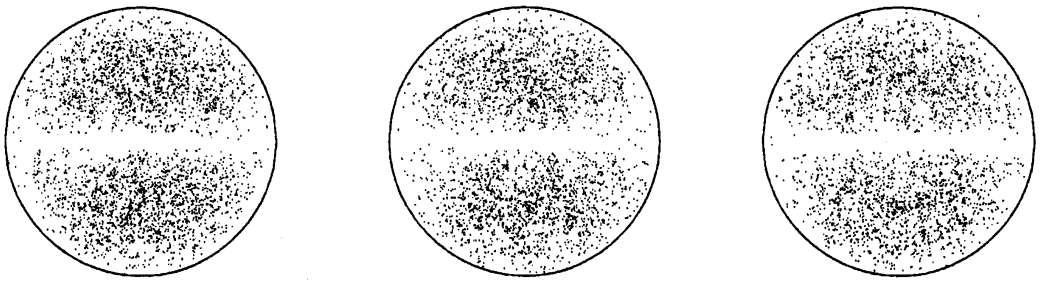

(a) (b) (c)

Figure 6: Poincaré sections based on $M_{l_1/2}$. $\alpha = 0.5$ and $\beta = 0.03$. (a) $a = 1.85$, (b) $a = 2.33$, (c) $a = 3.0$. The initial locations of fluid particles and the period of plotting are the same as Fig.4.

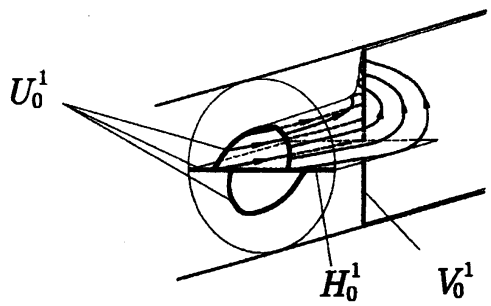

Figure 7: A schematic view of the lines of separation, U_0^1.

two sets:

$$H_{z_0}^n = \{(r,\theta,z)|0<r<1, \theta = 0,\pi, z = 2,4,\cdots,2n\}, \tag{13}$$

$$V_{z_0}^n = \begin{cases} \{(r,\theta,z)|0<r<1, \theta = \frac{\pi}{2},\frac{3\pi}{2}, z = l_1, l_1+2,\cdots,l_1+2(n-1)\} \\ \qquad\qquad \text{for} \quad z_0 < l_1, \\ \{(r,\theta,z)|0<r<1, \theta = \frac{\pi}{2},\frac{3\pi}{2}, z = l_1, l_1+2,\cdots,l_1+2n\} \\ \qquad\qquad \text{for} \quad z_0 > l_1. \end{cases} \tag{14}$$

These are the positions of the leading edges of horizontal and vertical plates within n periods from $z = z_0$. Then, we define the lines of separation, $U_{z_0}^n$, as

$$U_{z_0}^n = \left\{(r,\theta)| \lim_{t\to\infty} \boldsymbol{x}(t) \in H_{z_0}^n \text{ or } V_{z_0}^n,\ \boldsymbol{x}(0) = (r,\theta,z_0), z(t) \neq z_0 \text{ for } t>0\right\}. \tag{15}$$

Hence, the fluid particles starting from $U_{z_0}^n$ reach one of the leading edges in n periods from $z = z_0$. A schematic view of the lines of separation is given in Fig.7. In principle, exact numerical calculation of $U_{z_0}^n$ is impossible because it needs to take the limit of $t \to \infty$. Here we calculate it approximately by integrating Eq.(10) in backward time direction from the lines located slightly apart from the leading edges, and collecting the cross-sectional positions of them at $z = z_0$. In this way, we need to restrict the calculation time to a finite value T_{cal} since there exist particles which cannot reach at $z = z_0$ in a finite time. We here choose $T_{cal} = 30$. Figure 8 shows the lines of separation $U_{l_1/2}^1$ for some sets of values of parameters. From the definition, the ends of a line of separation are attached to the cylindrical wall, a plane plate or another line of separation. Furthermore, the lines do not cross each other. However, the lines in Fig.8 do not satisfy these conditions strictly because of the finite calculation time. The total length of these lines grows as β increases, because the effect of the wall rotation become stronger as β increases, and then fluid is stretched more strongly in the cross-sectional direction. Furthermore, by comparing the distribution of the lines of separation with the corresponding Poincaré sections, it is found that the lines exist only within the chaotic region. The reason for it is that islands on which map M_{z_0} should be continuous cannot contain the lines of separation because the map is discontinuous on them.

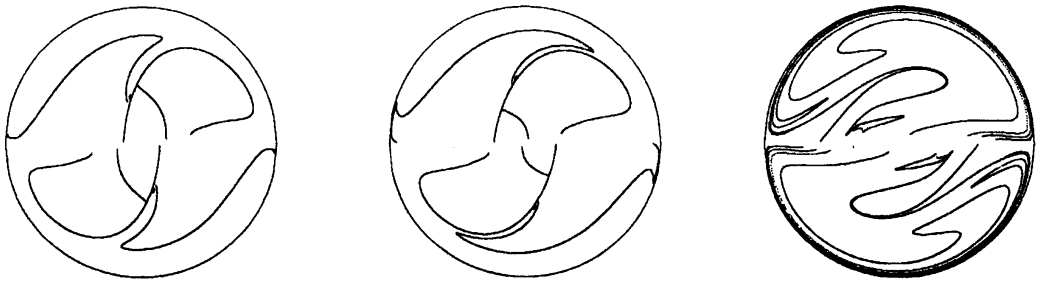

(a) (b) (c)

Figure 8: Lines of separation, $U^1_{l_1/2}$. $\alpha = 0.5$. (a) $\beta = 0.01$, $a = 1.0$, (b) $\beta = 0.01$, $a = 1.85$, (c) $\beta = 0.03$, $a = 1.85$. The initial positions of 40000 trajectories calculated here are uniformly placed on the lines 10^{-5} upstream from the leading edges.

We can recognize the close relation between the stretching of fluid elements and the lines of separation. Figure 9 shows the initial locations of blobs on $z = l_1/2$ and their evolutions in one period. Blobs whose initial locations are close to the lines of separation, such as Figs.9(a) and (b), are strongly stretched, whereas the blobs whose initial locations are not close to them, such as Fig.9(c), are only weakly stretched. We obtained the similar results in the calculations for different initial locations of blobs and the values of the parameters. Hence, we can conclude that only the blobs starting from the vicinity of the lines of separation are strongly stretched. Therefore, the separation by the leading edges of plates plays an important role in the mixing in PPM. The reason for the strong stretching of a fluid in the vicinity of the lines of separation is that they pass the regions of large strain rate along the cylindrical wall after the separation by a leading edge.

Khakhar et al. (1987) examined the residence time of each fluid particle defined as the time required for its movement over a specific period for the original PPM using the approximate velocity field, and found that the time of particles within the islands is usually considerably smaller than that of particles within the chaotic region. Although they considered the residence time for 5 periods, we here calculate the residence times for only one period, that is $T(r, \theta)$ in Eq.(11), in order to examine their distribution within the chaotic region. Since the residence time of particles which pass very close to the rigid wall and wandering between neighboring elements due to the backward flow can be infinite, we consider only the residence time T satisfying $T < 30$. Figure 10 shows the contours of the residence time of particles whose initial positions are on $z = l_1/2$. The residence time takes relatively large values in the regions where the contours densely exist. From the comparison between this figure and Fig.8, we find that the residence time is large around the lines of separation. The reason for it is that a fluid particle starting from the position near the lines of separation travels slowly in the axial direction since they move along the rigid wall after passing by a leading edge. There is no difference in the residence time distribution between the islands and the chaotic region. The large

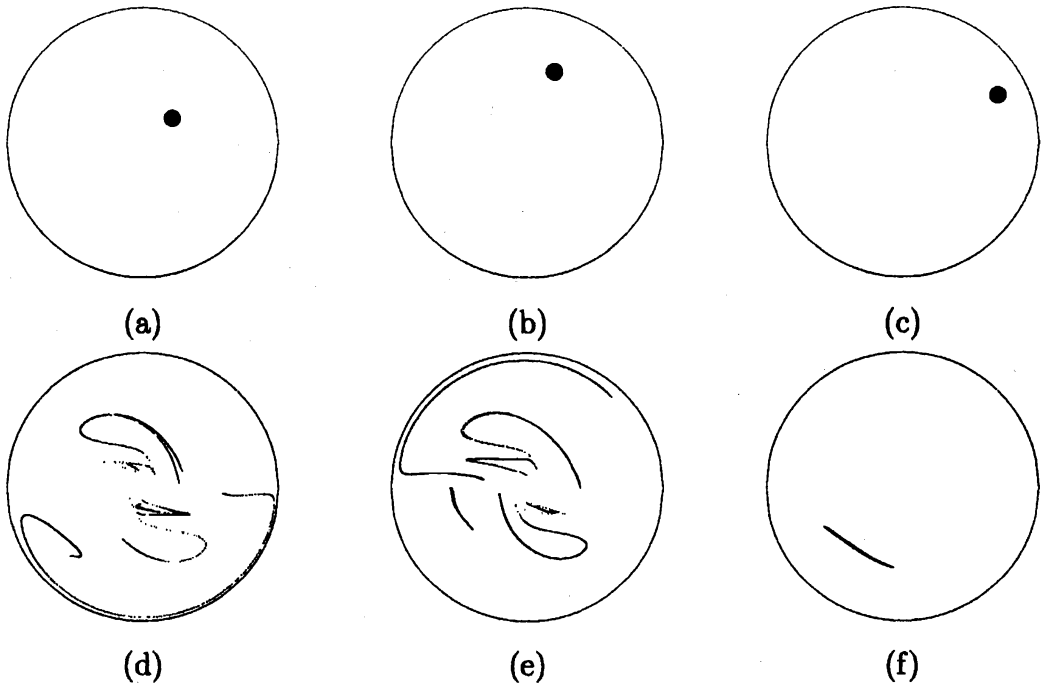

Figure 9: Time evolution of small blobs. Each blob has radius 0.06. $\alpha = 0.5$, $\beta = 0.03$, and $a = 1.0$. Blobs in (a) and (b) which are close to the lines of separation and that in (c) which is not close to the lines evolve to (d), (e) and (f), respectively.

difference in the residence time between islands and the chaotic region, seen in Khakhar et al. (1987) seems to be because they considered the residence time for 5 periods which is long enough for the lines of separation to spread over the chaotic region.

Finally, we shall see some numerical simulations of the time evolution of the dye injected constantly at the fixed location on $z = z_0$. Figure 11(a) shows the dye streak initially injected within a KAM-tube. We see that the dye travels in the axial direction, staying inside the tube. Because the period of the stable periodic orbit which cause the tube is 2, the streak comes back to the injected position after 2 period. The dye streak initially injected on $U^1_{l_1/2}$ is shown in Fig.11(b). The dye is only slightly stretched until it is

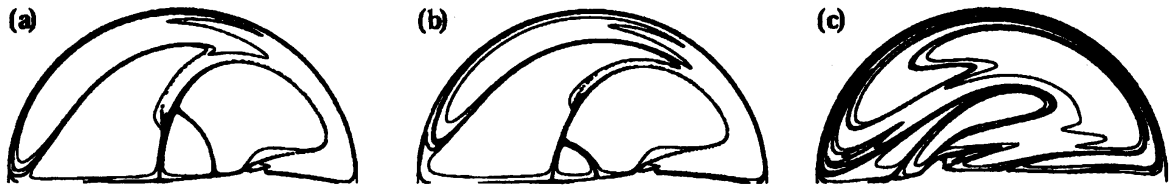

Figure 10: Contours of the residence time based on the 98500 trajectories starting from the initial positions on $z = l_1/2$. The initial positions are on square grid points of interval 0.01 on the upper part of the cross-section. $\alpha = 0.5$. (a) $\beta = 0.01$, $a = 1$, (b) $\beta = 0.01$, $a = 1.85$, (c) $\beta = 0.03$, $a = 1.85$.

separated by the first leading edge of the horizontal plate. After the separation, it travels slowly along the plate, and then is strongly stretched in the cross-sectional direction along the cylindrical wall. In Fig.11(c), the dye streak (grey) within the chaotic region whose injected position is not close to $U^1_{l_1/2}$ and the streak (black) within the KAM-tube are shown together. The grey dye travels in the axial direction without strong stretching as well as the black dye. The difference between their evolutions arises when the grey dye is suddenly stretched after the separation by the leading edge of the second horizontal plate. These observations confirm the close relation between the mixing within the chaotic region and the lines of separation.

4 Conclusions

We numerically calculated the exact velocity field of the PPM system, and examined the mixing of a fluid in this system. We then found that increasing the relative strength, β, of the wall rotation to that of pressure gradient in the axial direction or changing the ratio, a, of the lengths of neighboring plates can shrink or erase tubular invariant sets of trajectories which is a major obstacle to the mixing. This result qualitatively coincides with that in the previous studies.

Furthermore, we examined the mixing process within the chaotic region, by introducing the lines of separation similarly to Mizuno and Funakoshi (2002). From the facts that a blob initially close to the lines of separation is strongly stretched in the cross-sectional direction after it is separated by a leading edge and that only the regions of large strain rate near the cylindrical wall contributes the stretching in the cross-sectional direction, we can expect efficient mixing in a few periods within the chaotic region where the lines of separation for the corresponding periods spread over.

On the residence time of fluid particles, Khakhar et al. (1987) found that fluid particles within the tubular invariant sets travels in the axial direction relatively faster than the particles outside them by calculating the residence time for 5 periods. We here examined their distribution within chaotic region, considering only one period. We then found that the residence time for particles starting from a vicinity of the lines of separation is longer than those for the initial positions located apart from the lines of separation. Provided that the lines of separation spread over the chaotic region if the considered number of the periods, n, is large enough, we expect to obtain the same distribution as in Khakhar et al..

From the observation of the time evolution of the dyes for different initial positions, we found that fluid inside of KAM-tubes and fluid whose initial position is not close to the lines of separation make the similar motion, that is, fast traveling in the axial direction without strong stretching in the cross-sectional direction. The difference is that fluid

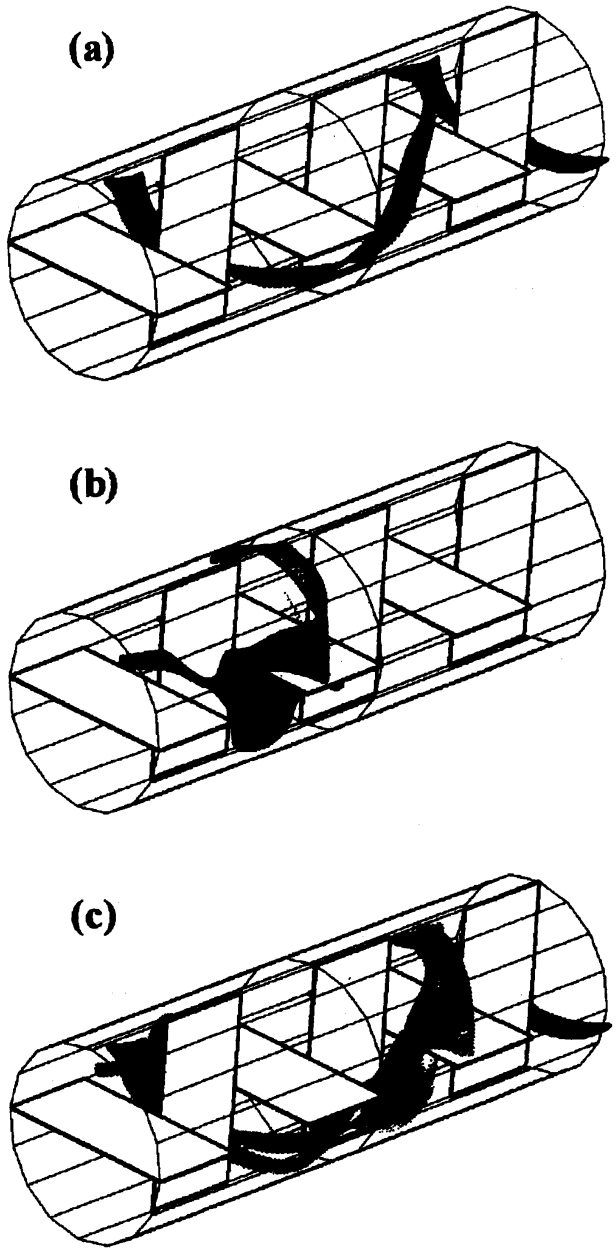

Figure 11: Dye streaks for different initial positions on $z = l_1/2$. $\alpha = 0.5$, $\beta = 0.03$ and $a = 1.0$. Each blob is injected constantly at each initial position since $t = 0$. 600 particles approximating each dye are initially placed within the circle of radius 0.06 centered at (a) $(r\cos\theta, r\sin\theta) = (0, 0.75)$, (b) $(0, 0.4)$, (c) $(-0.35, 0.5)$. (a) is the dye streak at $t = 20$ injected within a KAM-tube. (b) is the dye streak at $t = 10$ injected on $U^1_{l_1/2}$. (c) is the dye streak (grey) at $t = 16$ injected within the chaotic region not on $U^1_{l_1/2}$, which is shown with the streak (black) in (a).

elements within the chaotic region are suddenly stretched just after the separation by a leading edge.

References

Aref, H., 1990. Chaotic advection of fluid particles. Phil. Trans. R. Soc. Lond., A 333, 273-288.

Ferziger, J.H. and Perić, M., 1999. Computational methods for fluid dynamics. Springer.

Franjione, J.G. and Ottino, J.M., 1992. Symmetry concepts for the geometric analysis of mixing flows. Phil. Trans. R. Soc. Lond., A 338, 301-323.

Khakhar, D.V., Franjione, J.G. and Ottino, J.M., 1987. A case study of chaotic mixing in deterministic flows: the partitioned-pipe mixer. Chem. Eng. Sci., 42, 2909-2926.

Kusch, H.A. and Ottino, J.M., 1992. Experiments on mixing in continuous chaotic flows. J. Fluid Mech., 236, 319-348.

Ling, F.H., 1993. Chaotic mixing in a spatially periodic continuous mixer. Phys. Fluids, A 5, 2147-2160.

Meleshko, V.V., Galaktionov, O.S., Peters, G.W.M. and Meijer, H.E.H., 1999. Three-dimensional mixing in Stokes flow: the partitioned pipe mixer problem revisited. Eur. J. Mech. B/Fluids, 18, 783-792.

Mizuno, Y. and Funakoshi, M., 2002. Chaotic mixing due to a spatially periodic three-dimensional flow. Fluid Dyn. Res., 31, 129-149.

Muzzio, F.J., Swanson, P.D. and Ottino, J.M., 1991. The statistics of stretching and stirring in chaotic flows. Phys. Fluids, A3, 822-834.

Ottino, J.M., 1989. The kinematics of mixing: stretching, chaos and transport. Cambridge University Press.

Ottino, J.M., 1990. Mixing, chaotic advection, and turbulence. Annu. Rev. Fluid Mech., 22, 207-253.